



BEHAVIOR OF STRUCTURES ISOLATED USING VFPI DURING NEAR SOURCE GROUND MOTIONS

Pranesh MURNAL¹ and Ravi SINHA²

SUMMARY

Earthquakes affecting urban areas in the recent past have clearly demonstrated the vulnerability of urban building stock to ground motions. A large number of engineered buildings designed and constructed using modern techniques have been damaged. Several modern vibration control techniques using base isolation have been proposed in published literature to provide seismic resistance, some of which have also been implemented successfully. However most of these isolation devices are of limited effectiveness under near-source ground motions due to pulse-type characteristics of such excitations. A recently proposed sliding isolation system, known as the variable frequency pendulum isolator (VFPI) has unique characteristics that help overcome the limitations of traditional isolation system for near source ground motions. The VFPI incorporates isolation, energy dissipation as well as restoring force mechanisms in a single unit, and has additional advantages due to response-dependent variable frequency of oscillation and bounded restoring force. Isolator parameters of VFPI can be chosen to obtain the desired rate of time-period variation as well as initial time period. In this paper, behavior of structures isolated using VFPI subjected to near source ground motions has been numerically examined. Response of typical structural systems isolated with VFPI and other isolation systems under near-source ground motions have been investigated. The traditional isolation systems are found to be of limited effectiveness in reducing the response of structures while VFPI show significant reduction in response.

INTRODUCTION

Use of base isolation systems has emerged as a very effective technique for aseismic design of structures. In base isolation technique, a flexible layer (or isolator) is placed between the structure and its foundation such that relative deformations are permitted at this level. Due to flexibility of the isolator layer, the time period of motion of the isolator is relatively long; as a result the use of isolator shifts the fundamental period of the structure away from the predominant periods of ground excitation. Extensive review of base isolation systems and its applicability is available in literature (Buckle and Mayes [1], Kelly [2], and Naeim and Kelly [3]).

¹ Professor, Department of Applied Mechanics, Government College of Engineering, Karad, Maharashtra, India. Email: pmurnal@yahoo.com

² Professor, Department of Civil Engineering Indian Institute of Technology Bombay, India. Email: rsinha@civil.iitb.ac.in

Practical isolation devices typically also include energy dissipating mechanism so as to reduce deformations at the isolator level. For example friction type base isolators like Pure-Friction System (horizontal sliding surface) have been found to be very effective in reducing structural response (Mostaghel et al. [4]). The performance of friction isolators is relatively insensitive to variations in the frequency content and amplitude of the input excitation, making performance of sliding isolators very robust. Pure-Friction (PF) system may experience large sliding and residual displacements, which are often difficult to incorporate in structural design. An effective mechanism to provide restoring force by gravity has been utilized in Friction Pendulum System (FPS) (Zayas et al. [5]). In this system, the sliding surface takes a concave spherical shape so that the sliding and re-centering mechanisms are integrated in one unit. One main disadvantage is that FPS isolators can be effectively designed for a specific level (amplitude and frequency characteristics) of ground excitation (Sinha and Pranesh [6]).

The authors have recently developed a new isolator called the Variable Frequency Pendulum Isolator (VFPI) that incorporates the advantages of both the FPS and PF isolators (Pranesh and Sinha [7], Pranesh and Sinha [8]). The most important properties of this system are: (1) its time period of oscillation depends on sliding displacement, and (2) its restoring force has a bounded value and exhibits softening behavior. Recent investigations systems have shown VFPI to be very effective for a variety of excitation and structural characteristics.

The study of structures subjected to near-field ground motions has a special significance due to the nature of such ground motions. Near field ground motions are characterized by pulse type excitations having narrow range of frequencies. Behavior of most base isolated structures subjected to near-field ground motions is not satisfactory due to this nature of ground motion. In the present paper the performance of VFPI for aseismic design of multi-degree-of-freedom (MDOF) structures subjected to near-field ground motions has been investigated. The effectiveness of VFPI in comparison with the other frictional base isolation systems has been examined.

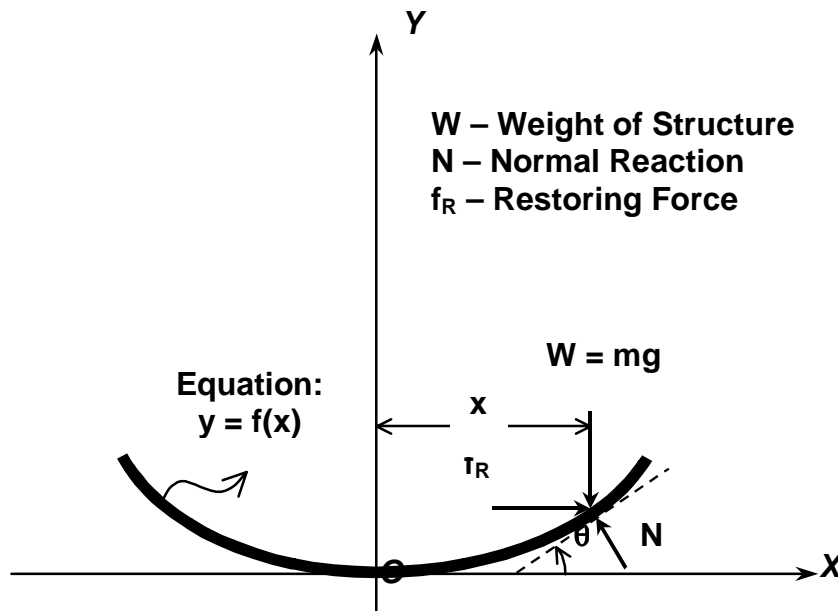


Figure 1. Free body diagram of smooth sliding surface of isolator.

VFPI DESCRIPTION

Consider the motion of a rigid block of mass m sliding on a smooth curved surface of defined geometry, $y = f(x)$ as shown in Fig. 1. At any instant the horizontal restoring force due to weight of the structure is given by

$$f_R = mg \frac{dy}{dx} \quad (1)$$

Assuming that the restoring force is mathematically represented by an equivalent non-linear mass-less horizontal spring, the spring force can be expressed as the product of the equivalent spring stiffness and the deformation, i.e.,

$$f_R = k(x)x \quad (2)$$

where $k(x)$ is the instantaneous spring stiffness, and x is the sliding displacement of the mass. If the mass is modeled as a single-degree-of-freedom oscillator, the spring force (restoring force) can be expressed as the product of the total mass of the system and square of oscillation frequency

$$f_R = m\omega_b^2(x)x \quad (3)$$

Here, $\omega_b(x)$ is the instantaneous isolator frequency, and depends solely on the geometry of sliding surface. In Friction Pendulum System, which has a spherical sliding surface, this frequency is almost constant and is approximately equal to $\sqrt{g/R}$, where R is the radius of curvature of the sliding surface (Zayas et al. [9]).

Sliding surface based on the expression of an ellipse has been used as the basis for developing sliding surface of VFPI (Pranesh [10]). The equation of an ellipse with a and b as its semi-major and semi-minor axes, respectively, and with co-ordinate axes as shown in Fig. 1 is given by,

$$y = b(1 - \sqrt{1 - x^2/a^2}) \quad (4)$$

The expression for frequency of elliptical surface is given by

$$\omega_b^2(x) = \omega_i^2 / \sqrt{1 - x^2/a^2} \quad (5)$$

where $\omega_i^2 = b/a^2$ is the square of initial frequency. From this expression it is observed that the frequency of the surface is inversely proportional to the square of semi-major axis. So to get the desired variation of the frequency, the semi-major axis is expressed as a variable to obtain the geometry of VFPI. The semi-major axis has been expressed as

$$a = x + d \quad (6)$$

Substituting this in the equation of an ellipse with origin as shown in Fig. 1, the expression for geometry of sliding surface of VFPI is obtained as

$$y = b \left[1 - \frac{\sqrt{d^2 + 2dx \operatorname{sgn}(x)}}{d + x \operatorname{sgn}(x)} \right] \quad (7)$$

where $\operatorname{sgn}(x)$ is the signum function introduced for maintaining symmetry of sliding surface about the central vertical axis. This assumes a value of $+1$ for positive sliding displacement and -1 for negative sliding displacement. The slope at any point on this sliding surface is given as

$$\frac{dy}{dx} = \frac{bd}{(d + x \operatorname{sgn}(x))^2 \sqrt{d^2 + 2dx \operatorname{sgn}(x)}} x \quad (8)$$

To simplify the notations, a non-dimensional parameter $r = x \operatorname{sgn}(x)/d$ has been used. By substituting r and the initial frequency $\omega_i^2 = gb/d^2$ in (4), and combining with (1) and (2), the isolator frequency at any sliding displacement can be expressed as

$$\omega_b^2(x) = \frac{\omega_I^2}{(1+r)^2 \sqrt{1+2r}} \quad (9)$$

In the above equations, parameters b and d completely define the isolator characteristics. It can be observed that the ratio b/d^2 governs the initial frequency of the isolator. Similarly, the value of $1/d$ determines the rate of variation of isolator frequency, and this factor has been defined as frequency variation factor (FVF). The profile of sliding surface and variation of oscillation frequency of a typical VFPI with respect to the sliding displacement is shown in Figs. 2(a) and (b), respectively. For comparison purposes, the oscillation frequency of FPS with same initial frequency has also been shown, which is found to be almost constant. From this plot it is seen that the oscillation frequency of VFPI decreases with increasing sliding displacement and asymptotically approaches zero. The rate of decrease can be controlled by the value of FVF parameter. The force-deformation hysteresis for example FPS and VFPI are shown in Fig. 2(c). It can be observed that the isolator force in VFPI first increases to reach its maximum value, and later slowly decreases so as to asymptotically approach the frictional force at large sliding displacement. This is an important property of VFPI, which limits the force transmitted to the structure.

MATHEMATICAL FORMULATION

Consider an N-story shear structure isolated by sliding type isolator. The motion of the structure can be in either of two phases: non-sliding phase and sliding phase. In non-sliding phase, the structure behaves like a conventional fixed base structure since there is no relative motion at the isolator level. When the frictional force at the sliding surface is overcome, there is relative motion at the sliding surface, and the structure enters sliding phase. The total motion consists of a series of alternating non-sliding and sliding phases.

Non-sliding Phase

In non-sliding phase the structure behaves as a fixed-base structure, since there is no relative motion between the ground and base mass. The equations of motion in this phase are:

$$\mathbf{M}_0 \ddot{\mathbf{x}}_0 + \mathbf{C}_0 \dot{\mathbf{x}}_0 + \mathbf{K}_0 \mathbf{x}_0 = -\mathbf{M}_0 \mathbf{r}_0 \ddot{x}_g \quad (10)$$

and

$$x = \text{constant}; \quad \dot{x}_b = \ddot{x}_b = 0 \quad (11)$$

where, \mathbf{M}_0 , \mathbf{C}_0 and \mathbf{K}_0 are the mass, damping and stiffness matrices of the fixed-base structure, respectively, $\mathbf{x}_0 = [x_1, x_2, \dots, x_N]^T$ is the vector of displacements of the degrees of freedom (DOFs) of the superstructure relative to the base mass (excluding the DOF of base mass), x_b is the displacement of the base mass (m_b) relative to the ground, x_g is the ground displacement, \mathbf{r}_0 is the influence coefficient vector and over-dot indicates derivative with respect to time. Since the base mass does not move relative to the ground, the velocity and acceleration of the base relative to the ground are zero. However the sliding displacement may be non-zero. The structure is classically damped in this phase and hence (10) can be readily solved by usual modal analysis procedures (Clough and Penzien [11]).

Initiation of Sliding Phase

When the structure is subjected to base excitation, it will remain in non-sliding phase unless the frictional resistance at the sliding surface is overcome. Therefore the condition for the beginning of sliding phase can be written as

$$\left| \left\{ \sum_{i=1}^N m_i (\ddot{x}_i + \ddot{x}_g) + m_b \ddot{x}_g \right\} + m_i \omega_b^2(x) x_b \right| \geq m_i \mu g \quad (12)$$

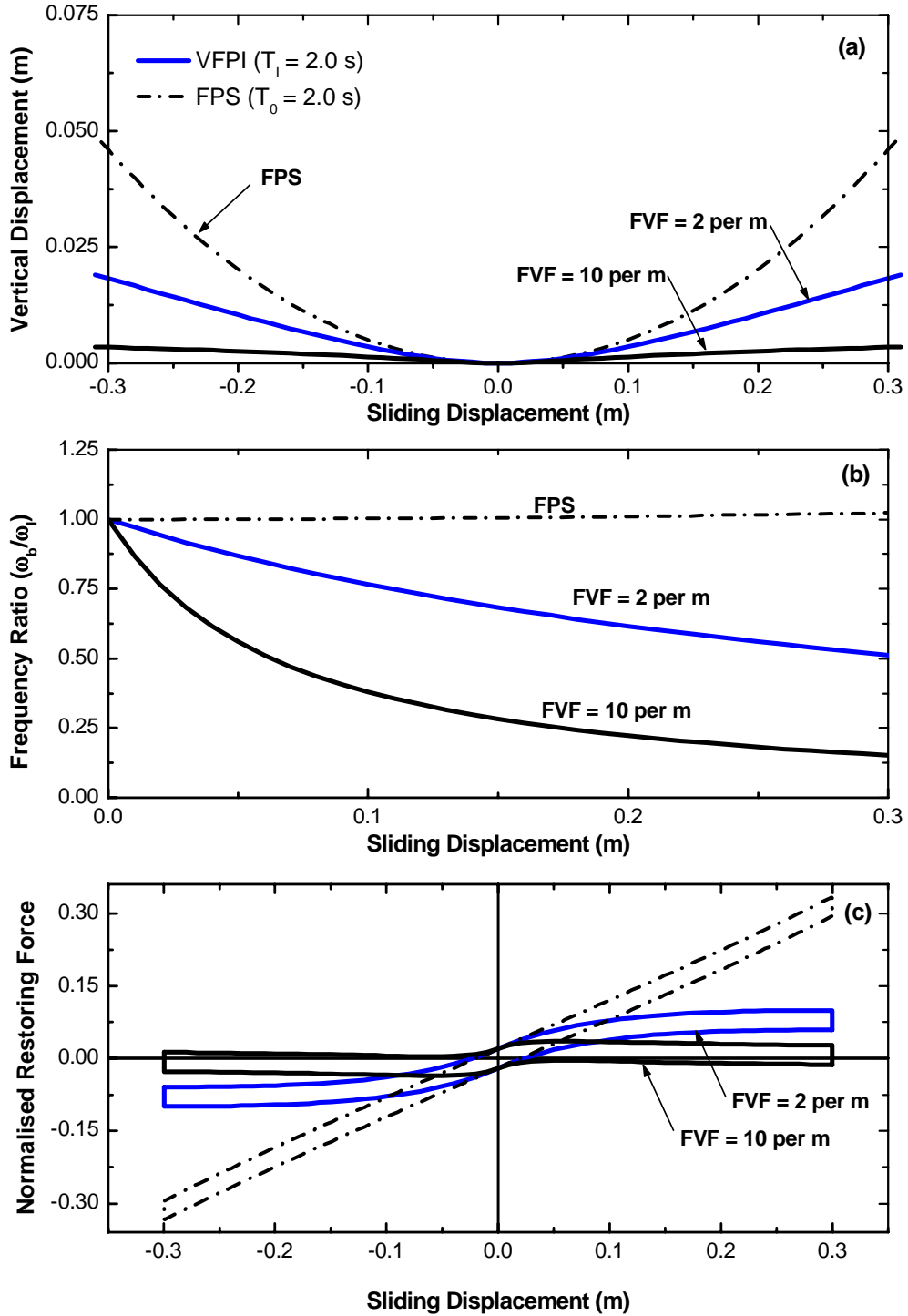


Figure 2. Properties of VFPI and FPS for different geometrical parameters ($\mu = 0.02$, $T_1 = 2.0$ s) (a) Sliding Surface Profile, (b) Frequency Variation, and (c) Hysteresis Curves.

Sliding Phase

Once the inequality (12) is satisfied the structure enters sliding phase and the degree of freedom (DOF) corresponding to the base mass also experiences motion. The equations of motion are now given by

$$\mathbf{M}\ddot{\mathbf{x}} + \mathbf{C}\dot{\mathbf{x}} + \mathbf{K}\mathbf{x} = -\mathbf{M}\mathbf{r}\ddot{x}_g - \mathbf{r}\mu_f \quad (12)$$

where, \mathbf{M} , \mathbf{C} , \mathbf{K} are the modified mass, damping and stiffness matrices of order $N+1$, \mathbf{r} is the modified influence coefficient vector and μ_f is the frictional force as given below.

$$\mathbf{M} = \begin{bmatrix} \mathbf{M}_0 & \mathbf{M}_0\mathbf{r}_0 \\ [\mathbf{M}_0\mathbf{r}_0]^T & m_t \end{bmatrix}, \quad \mathbf{C} = \begin{bmatrix} \mathbf{C}_0 & \mathbf{0} \\ \mathbf{0} & 0 \end{bmatrix}, \quad (13)$$

$$\mathbf{K} = \begin{bmatrix} \mathbf{K}_0 & \mathbf{0} \\ \mathbf{0} & k_b \end{bmatrix}, \quad \mathbf{x} = \begin{Bmatrix} \mathbf{x}_0 \\ x_b \end{Bmatrix}, \quad \mathbf{r} = \begin{Bmatrix} \mathbf{0} \\ 1 \end{Bmatrix} \quad \text{and} \quad \mu_f = m_t g \mu \operatorname{sgn}(\dot{x}_b)$$

Equation (12) can be solved numerically. But for large size problems the computational effort is large and the analysis does not provide proper insight into the behavior of the structure. In view of this and the non-classical nature of damping, complex modal analysis is used in the present investigations.

Direction of Sliding

The direction of sliding depends on the signum function that in turn depends on the forces acting on the structure at the end of the previous non-sliding phase. Once inequality (12) is satisfied, the structure starts sliding in a direction opposite to the direction of the sum of total inertia force and restoring force at the isolator level. So, we have

$$\operatorname{sgn}(\dot{x}_b) = - \frac{\left[\sum_{i=1}^N m_i (\ddot{x}_i + \ddot{x}_b + \ddot{x}_g) \right] + m_b (\ddot{x}_b + \ddot{x}_g) + m_t \omega_b^2 x_b}{\left[\sum_{i=1}^N m_i (\ddot{x}_i + \ddot{x}_b + \ddot{x}_g) \right] + m_b (\ddot{x}_b + \ddot{x}_g) + m_t \omega_b^2 x_b} \quad (14)$$

The signum function remains unchanged in a particular sliding phase. The end of a sliding phase is governed by the condition that the sliding velocity of the base mass is equal to zero, i.e.,

$$\dot{x}_b = 0 \quad (15)$$

Once the sliding velocity is zero, the structure may enter a non-sliding phase, reverse its direction of sliding, or have a momentary stop and then continue in the same direction. To determine the correct state, the solution process needs to continue using equations of non-sliding phase wherein the sliding acceleration is forced to zero and the validity of the inequality (12) is checked. If this inequality is satisfied at the same instant of time when the sliding velocity is zero, it shows that there is a sudden stop at that instant.

ENERGY BALANCE

Base isolators reduce structural response by filtering the seismic excitations and by dissipating energy thereby reducing the energy that needs to be dissipated by the structure. Often it is very difficult to decide a proper trade-off between structural deformations and isolator displacements for determination of isolator properties. The energy quantities are convenient to consider since they involve all the response quantities and hence represent overall response of the structure. As they are scalar, only a single energy equation for the entire structure can be derived irrespective of the number of degrees of freedom in the structure. So, the energy quantities can represent the isolator performance in a more unified manner and can be used to decide the overall performance of the isolator.

The energy balance at any instant can be easily derived by calculating the total work done by all conservative and non-conservative forces up to that instant. This can be achieved by calculating the differential work done by all the forces during a small deformation of the structure $d\mathbf{x}_0$, and then integrating to get the total work done. The final expression for the energy balance is found to be

$$\begin{aligned} & \frac{1}{2} \dot{\mathbf{x}}_0^T \mathbf{M}_0 \dot{\mathbf{x}}_0 + \frac{1}{2} m_b \dot{x}_b^2 + m_t g y + \frac{1}{2} \mathbf{x}_0^T \mathbf{K}_0 \mathbf{x}_0 + \int [\dot{\mathbf{x}}_0^T \mathbf{C}_0 \dot{\mathbf{x}}_0] dt + \\ & \int m_t \mu g \operatorname{sgn}(\dot{x}_b) dx_b = \int [\dot{\mathbf{x}}_0^T \mathbf{M}_0 \mathbf{r}_0] dx_g + \int m_b \ddot{x}_b dx_g \end{aligned} \quad (16)$$

Equation (17) is similar to the absolute energy equation derived for the conventional MDOF structure in published literature, except for the additional terms involving the potential energy due to rising of the structure along the curved surface (third term in (16)) and the non-conservative energy term due to friction (sixth term in (16)) (Uang and Bertero [12]). There is no energy dissipation due to sliding friction during the non-sliding phase. Equation (16) can be written in short as

$$E_k + E_r + E_s + E_\xi + E_\mu = E_i \quad (17)$$

where E_k is the sum of absolute kinetic energies of all the masses, E_r and E_s are the restorable potential energy due to rising of the structure along the sliding surface of the isolator and elastic energy due to structural deformations, respectively. E_ξ and E_μ are the energy dissipated due to structural damping and sliding friction respectively. As the sum of frictional force and the restoring force is identical to the total inertia force, the term E_i on RHS is the absolute input energy.

RESPONSE OF EXAMPLE STRUCTURE

The effectiveness of VFPI to reduce response of an example MDOF structure subjected to near-field earthquake excitations has been presented in this section. The example structure is a five-story shear structure. The example building is represented as a lumped mass model with equal lumped mass of 60080 kg and equal story stiffness of 112600 kN/m for each floor. The frequencies and modal properties for the fixed-base and isolated structures are given in Table 1. Since the natural frequencies of a structure isolated by VFPI change continuously with the isolator sliding displacement, the frequencies shown in Table 1 thus indicate the upper bound on the frequencies when the isolator displacement is zero.

Table 1. Modal properties of fixed-base and isolated structures.

Mode	Isolator	1	2	3	4	5
Fixed – Freq. (Hz)	-	1.96	5.72	9.02	11.59	13.22
Eff. Modal Mass (%)	-	87.95	8.72	2.42	0.75	0.16
Isolated – Freq. (Hz)	0.49	3.64	6.92	9.76	11.93	13.31
Eff. Modal Mass (%)	99.93	0.07	0.00	0.00	0.00	0.00

The example structure is analyzed for ten near field ground motions. The details of the ground motions are presented in Table 2. These ground motions are derived from historical recordings. The ground motions chosen cover a wide variety of near field ground motions having different peak ground acceleration (PGA), frequency composition and duration. Using the formulation presented in the paper, time history analysis is carried out for the structure isolated by VFPI. The VFPI chosen in this study has an initial isolator time period of 2.0 s and FVF equal to 5.0 per m. The corresponding values of isolator parameters b and d are 0.04 m and 0.20 m, respectively. To investigate the effectiveness of VFPI, the responses are compared with those of structure is isolated with FPS and PF isolators. The FPS has been chosen with radius of 1.0 m so that its time period is around 2.0 s (equal to the initial period of the example VFPI). Coefficient of friction is assumed to be equal to 0.02. The structural damping is assumed as 5% of critical for all modes.

The response quantities are evaluated by solution of the equations of motion as discussed in the preceding sections. The main response quantities of interest are acceleration of top story, sliding displacement of isolator. Time-history plots for these response quantities of the example structure are subject to Northridge (Rinaldi) 1994 excitation are shown in Fig. 3. The maximum response values are also shown. It is seen from Fig. 3(a) that there is substantial reduction in the base shear for structure isolated by VFPI

throughout the time history, when compared to that isolated by FPS. This is due to the bounded restoring force characteristics of VFPI, which results in lesser forces transmitted to the structure. It is also observed from Fig. 3(b) that the accelerations in the structure are substantially lesser in VFPI-isolated structure than that isolated by other isolation systems. These plots clearly demonstrate the effectiveness of VFPI in comparison with conventional FPS and PF system. From Fig. 3(c), it is observed that the sliding displacements in case of VFPI increase and are even more than PF system. This is due to the fact that the isolator force in VFPI can act either as restoring or driving force depending on the direction of motion whereas in the PF system the constant frictional force always opposes the motion. However the residual displacements in VFPI are very small and are close to those of FPS, which clearly shows the effectiveness of the restoring mechanism in spite of large sliding displacements. From these response characteristics, it is therefore found that VFPI retains the main advantages of both FPS and PF isolators.

Table 2. Details of earthquake records used during numerical simulations.

S. No.	Name of earthquake	Designation	Magnitude	Distance of source (km)	PGA (g)	Duration (sec.)
1	Tabas, 1978	NFR-01	7.4	1.2	0.900	50
2	Loma Prieta, 1989, Los Gatos	NFR-02	7.0	3.5	0.718	25
3	Loma Prieta, 1989, Lex. Dam	NFR-03	7.0	6.3	0.686	40
4	C. Mendocino, 1992, Petrolia	NFR-04	7.1	8.5	0.638	60
5	Erzincan, 1992	NFR-05	6.7	2.0	0.432	21
6	Landers, 1992	NFR-06	7.3	1.1	0.713	50
7	Nothridge, 1994, Rinaldi	NFR-07	6.7	7.5	0.890	15
8	Nothridge, 1994, Olive View	NFR-08	6.7	6.4	0.732	60
9	Kobe, 1995	NFR-09	6.9	3.4	1.088	60
10	Kobe, 1995, Takatori	NFR-10	6.9	4.3	0.786	40

The maximum response of the example structure subjected to ten near field ground motions has been presented in Table 3 for the three isolation systems. From these results it is seen that VFPI remains effective for a wide range of near-field excitation characteristics. The acceleration response of FPS is very large when compared to VFPI and PF systems for most of the excitations. But the sliding displacements in VFPI are substantially high. However the system comes to its original position in most cases as is seen from residual displacements.

The effectiveness of isolators can be better understood using energy quantities. Table 4 shows the input energy and conservative energy for the example system subjected to different ground motions. Input energy is a measure of effectiveness of isolation and conservative energy is the energy transmitted to the structure. The difference in the two is the energy dissipated. From Table 4 it is observed that the input energy and conservative energy in case of FPS is substantially high when compared with FPS and PF systems. This shows the effectiveness of VFPI.

CONCLUSIONS

The effectiveness of variable frequency pendulum isolator (VFPI) for vibration control of MDOF systems subjected to near field ground motions has been presented in this paper. A five-story shear structure has been analyzed for different near-field ground motions. From these investigations it is found that the VFPI is very effective in reducing the response of structures when compared to the FPS and PF isolators. The VFPI reduces the response substantially without losing the restoring capability thereby combining the advantages of both FPS and PF isolators.

Table 3. Response of example system for different near-field ground motion records.

S. No.	Earthquake Record	Maximum Structural Acceleration (g)			Maximum Sliding Displacement (m)			Residual Displacement (m)		
		VFPI	FPS	PF	VFPI	FPS	PF	VFPI	FPS	PF
1	NFR-01	0.217	0.875	0.178	1.641	0.620	0.726	0.002	0.002	0.293
2	NFR-02	0.203	13.33	0.189	1.342	0.989	0.810	0.275	0.040	0.360
3	NFR-03	0.166	2.088	0.164	1.274	0.848	0.902	0.982	0.004	0.834
4	NFR-04	0.222	0.865	0.150	1.271	0.616	0.767	0.000	0.000	0.653
5	NFR-05	0.144	0.798	0.134	0.470	0.583	0.528	0.005	0.203	0.078
6	NFR-06	0.198	0.364	0.189	2.404	0.305	1.037	2.251	0.000	0.505
7	NFR-07	0.177	0.838	0.200	0.597	0.587	0.628	0.007	0.284	0.497
8	NFR-08	0.144	0.958	0.137	0.573	0.648	0.661	0.001	0.001	0.502
9	NFR-09	0.190	1.435	0.154	0.775	0.766	0.457	0.000	0.004	0.087
10	NFR-10	0.195	6.345	0.155	0.685	0.973	0.801	0.011	0.235	0.171

Based on investigations of response of MDOF systems isolated by VFPI, the following conclusions can be drawn:

1. The VFPI is very effective in reducing the response of structures under variety of near-field ground excitations. The performance of VFPI is found to be robust and superior to that of FPS and PF isolators.
2. VFPI acts as an isolator combined with effective energy dissipation and restoring mechanism.

REFERENCES

1. Buckle, I. G., and Mayes, R. L. "Seismic isolation: history, application and performance - a world view." *Earthquake Spectra* 1990; 6(2): 161-201.
2. Kelly, J. M. "State-of-the-art and state-of-the-practice in base isolation." Seminar on Seismic Isolation, Passive Energy Dissipation and Active Control (ATC-17-1), Applied Technology Council, Redwood City, CA, USA 1993.
3. Naeim, F. and Kelly, J. M. "Design of seismic isolated structures: from theory to practice" John Wiley and Sons, New York, NY, USA 1993.
4. Mostaghel, N., Hejazi, M., and Tanbakuchi, J. "Response of sliding structures to harmonic support motion." *Earthquake Engineering and Structural Dynamics* 1983; 11(3): 355-366.
5. Zayas, V. A., Low, S. S., and Mahin, S. A. "The FPS earthquake resisting system: Experimental report." Report No. UCB/EERC-87/01, Earthquake Engineering Research Center, University of California, Berkeley, CA, USA 1987.
6. Sinha, R., and Pranesh, M. "FPS isolator for structural vibration control." Proc., International Conference on Theoretical, Applied, Computational and Experimental Mechanics (CD Volume), IIT Kharagpur, India 1998.
7. Pranesh, M., and Sinha, R. "Vibration control of primary-secondary systems using variable frequency pendulum isolator." Proc., 11th Symposium on Earthquake Engineering, University of Roorkee, Roorkee, India 1998; 697-704.
8. Pranesh M., and Sinha, R. "VFPI: An isolation device for aseismic design." *Earthquake Engineering and Structural Dynamics*, 2000; 29(5): 603-627.
9. Zayas, V. A., Low, S. S., and Mahin, S. A. "A simple pendulum technique for achieving seismic isolation." *Earthquake Spectra* 1990; 6(2): 317-333.
10. Pranesh, M. "VFPI: An innovative device for aseismic design." Ph.D. Thesis, Indian Institute of Technology, Bombay, India 2000.
11. Clough, R. W., and Penzien, J. "Dynamics of Structures." 2nd edition, McGraw-Hill, Inc., New York, NY, USA 1993.

12. Uang, C. M., and Bertero, V. V. "Evaluation of seismic energy in structures." Journal of Earthquake Engineering and Structural Dynamics 1990; 19(1): 77-90.

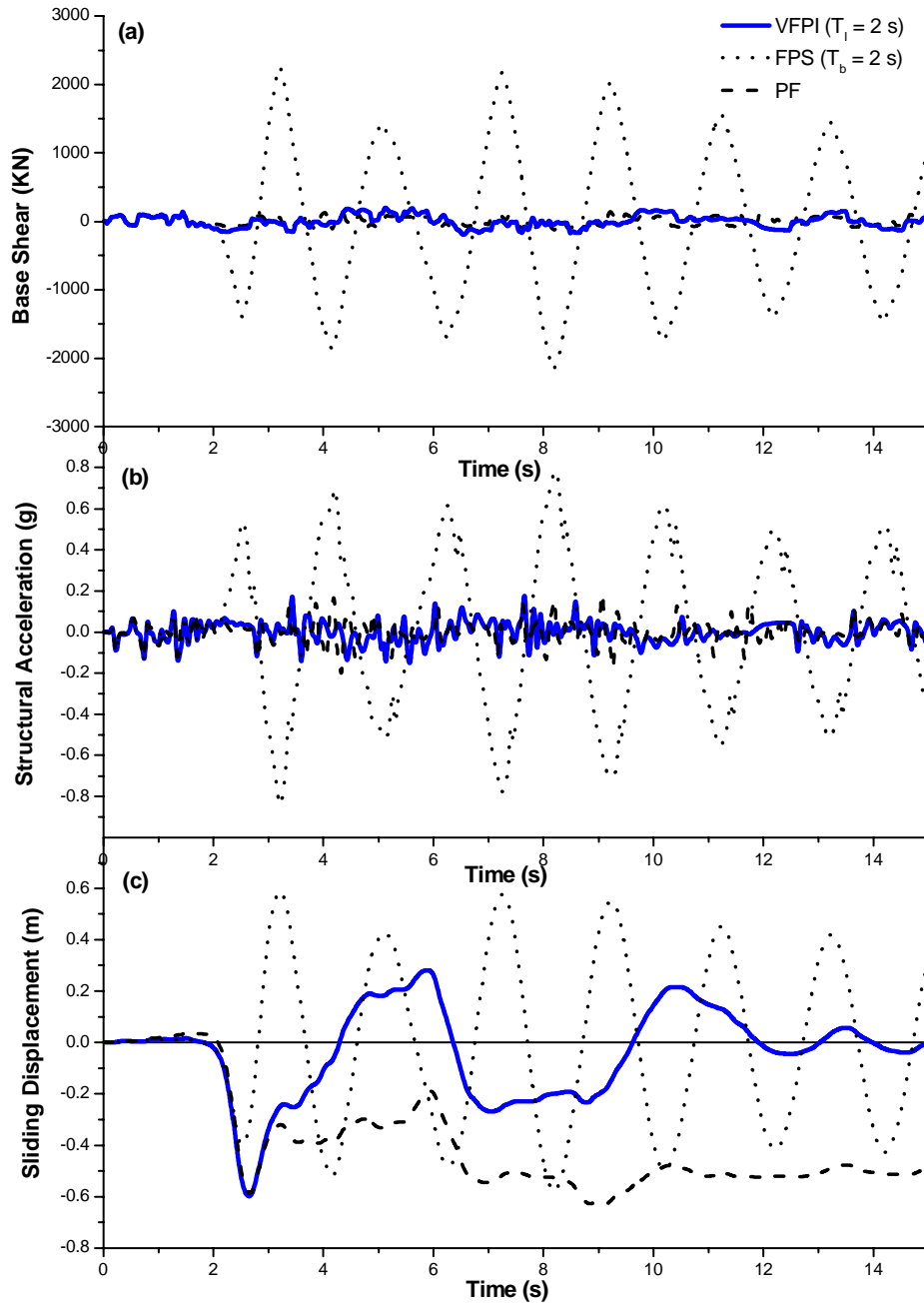


Figure 3. Time history response of example structure subjected to 1994 Northridge (Rinaldi) ground motions.

Table 4. Energy characteristics of example system subjected to various near-field ground motions.

S. No.	Earthquake Record	Input Energy (10^4 N.m)			Conservative Energy (10^4 N.m)		
		VFPI	FPS	PF	VFPI	FPS	PF
1	NFR-01	43.48	168.0	35.40	7.920	113.0	1.779
2	NFR-02	39.88	721.8	34.26	4.581	516.0	0.873
3	NFR-03	25.05	210.2	17.29	4.471	155.3	1.588
4	NFR-04	23.88	114.8	17.72	6.190	95.83	1.518
5	NFR-05	17.75	124.8	11.66	1.748	88.10	0.541
6	NFR-06	36.50	326.4	21.73	14.97	28.25	5.075
7	NFR-07	22.83	128.7	15.84	2.720	73.30	0.859
8	NFR-08	18.00	118.1	14.57	1.190	99.90	0.697
9	NFR-09	30.73	222.0	26.27	1.677	144.4	0.471
10	NFR-10	46.60	566.0	38.84	1.976	464.6	0.521